(14) O. Dann and P. Nickel, *Justus Liebigs Ann. Chem.*, **667**, 101 (1963).
(15) O. Stern and M. Volmer, *Phys. J.*, **20**, 183 (1919).
(16) P. Debye, *Trans. Electrochem. Soc.*, **82**, 265 (1942).
(17) Data were obtained at the Center for Fast Kinetics Research, University of Texas, Austin.
(18) Th. Forster, *Discuss. Faraday Soc.*, **27**, 7 (1959).
(19) D. N. Harpp and C. Heitner; *J. Am. Chem. Soc.*, **94**, 8179 (1972).
(20) The benzophenone-sensitized dimerization of MeTND was also studied in acetonitrile and the value of $\alpha = 0.32 \pm 0.05$ was derived.
(21) H. Morrison, P. Wells, and R. Hoffman, *J. Org. Chem.*, **36**, 102 (1971).
(22) S. P. Pappas and R. D. Zehr, Jr., *J. Am. Chem. Soc.*, **93**, 7112 (1971).
(23) An extensive discussion of biradicaloid geometries and the factors influencing energy partitioning in biradicals is available: J. Michl, *Photochem. Photobiol.*, **25**, 141 (1977).
(24) M. S. El Faghi El Amoudi, P. Geneste, and J. L. Olive, *Tetrahedron Lett.*, 999 (1978).
(25) (a) M. W. Wolf, R. E. Brown, and L. A. Singer, *J. Am. Chem. Soc.*, **99**, 526 (1977); (b) M-H Hui and W. R. Ware, *ibid.*, **98**, 4718 (1976); (c) Y. Taniguichi, Y. Nishina, and N. Mataga, *Bull. Chem. Soc. Jpn.*, **45**, 764 (1972).
(26) E. N. Karaulova, D. Sh. Meilanova, and G. D. Gal'pern, *J. Gen. Chem. USSR (Engl. Transl.)*, **30**, 3262 (1960); *Zh. Obshch. Khim.*, **30**, 3292 (1960).
(27) D. S. Rao and B. D. Tilak, *J. Sci. Ind. Res., Sect. B*, **18**, 77 (1959).
(28) P. J. Wagner and D. J. Buchek, *J. Am. Chem. Soc.*, **91**, 5090 (1969).
(29) B. F. Plummer, *Mol. Photochem.*, **6**, 241 (1974).
(30) B. F. Plummer, *J. Chem. Educ.*, **55**, 719 (1978).
(31) (a) G. F. Vesley and G. S. Hammond, *Mol. Photochem.*, **5**, 367 (1973); (b) *J. Am. Chem. Soc.*, **89**, 3482 (1967).
(32) W. M. Moore and M. Ketchum, *J. Am. Chem. Soc.*, **84**, 1368 (1962).
(33) S. Udenfriend, "Fluorescence Assays in Biology and Medicine", Academic Press, New York, 1962, pp 119–121.

Investigation of the Zeolite Catalyzed Alkylation of Toluene Using Carbon-13 Nuclear Magnetic Resonance

Michael D. Sefcik

Contribution from Monsanto Company, St. Louis, Missouri 63166.
Received April 10, 1978

Abstract: The role of alkali metal cation exchange in the catalytic synthesis of styrene monomer from methanol and toluene over X-type zeolites has been investigated by ^{13}C NMR. Catalytic materials were examined with respect to both their physical and chemical interactions with various substrates. The replacement of sodium cations by cesium alters the distribution of methanol thermolysis products and enhances the yield of styrene and ethylbenzene via a restricted transition-state selectivity. As identified from the ^{13}C NMR spectra, the predominant reaction of the NaX is the dehydration of methanol to dimethyl ether followed by aromatic substitution on the toluene to yield undesirable ring alkylation byproducts. Cracking competes favorably with dehydration on the CsX, thereby reducing the yield of dimethyl ether. The restricted mobility of aromatic adsorbates on the CsX, as indicated by the NMR line shape, suggests that ring alkylation is hindered by the presence of cesium cations in the adsorption cavity which sterically restrict the formation of transition states which lead to these products.

Introduction

The zeolite catalyzed alkylation of toluene by methanol or formaldehyde to form styrene and ethylbenzene has been studied in several laboratories.[1-7] Both Japanese[1] and Russian[2] workers have reported that X-type zeolites are more active than Y-type and that selectivity of the catalyst for alkylation is dependent on the zeolite cation. Freeman and Unland[4] reported that selectivity in the toluene + methanol reaction to styrene and ethylbenzene increased with alkali-metal cation size and that the borate-promoted, cesium-exchanged X zeolite was the most favorable of those studied.[5]

On the basis of laser Raman[4] and diffuse reflectance[6] measurements, Unland and Freeman and Unland concluded that the reaction selectivity was influenced by the electrostatic fields experienced by the aromatic nucleus. These interactions, primarily through perturbation of the π electrons, increased with loading level in a particular zeolite or with increasing cation size. Infrared studies[7] of the decomposition of methanol and formaldehyde on the Na, K, Rb, and Cs forms of X-type zeolites have shown that methoxide, carbonate, and formate species are formed in varying amounts and types on the different samples. The increased selectivity of these catalysts afforded by incorporation of borate into the zeolite is not understood. The failure of the borate to affect the adsorption of benzene has lead to the suggestion[4] that the borate may act on the methanol decomposition rather than the toluene activation in the toluene–methanol reaction.

The application of rare-spin nuclear magnetic resonance to the investigation of surface interactions of molecules has proven to be useful in elucidating the subtle dynamics of adsorbate-adsorbent interactions.[8-13] Analysis of the ^{13}C NMR line shapes provides information about the rotational freedom of molecules under the influence of surface interactions, while the wide chemical-shift range facilitates the identification of chemical intermediates and products formed during catalytic reactions. We have applied these techniques to the characterization of the dynamic interactions between various substrate molecules and a series of modified X zeolite materials which have been developed as catalysts for the synthesis of styrene monomer. With the results of this investigation we hope to explain the various catalytic properties of these modified molecular sieves, particularly the product distribution and relative yields.

Experimental Section

A. The Nuclear Magnetic Resonance Experiment. The carbon-13 pulsed Fourier transform nuclear magnetic resonance spectra of isotopically enriched compounds adsorbed on the molecular sieve samples were obtained on a modified Bruker spectrometer. The spectrometer operates at 22.6 MHz and is equipped with a time-shared external ^{19}F field-frequency stabilization system, a quadrature ^{13}C detector,[14] and a ^{13}C–^{1}H probe capable of accepting high power, long bursts of radio-frequency power at both the ^{13}C and ^{1}H Larmor frequencies without breakdown or cross talk. The spectrometer is free from base line artifacts.[15,16]

Three types of NMR experiments were performed in this study: scalar-decoupled Fourier transform (FT),[17] dipolar-decoupled Fourier transform,[18] and cross-polarization.[19] Scalar-decoupled FT NMR involves the application of a weak radio-frequency field ($\gamma H_2/2\pi$ = 3 kHz) to eliminate spin–spin coupling between the directly bonded carbons and protons. Scalar-decoupled FT NMR detects only those molecules which are rotating sufficiently fast ($>10^5$ Hz) to average the ^{1}H–^{13}C dipolar interactions to nearly zero. Dipolar-decoupled FT NMR, the second type of experiment performed in this study, requires

0002-7863/79/1501-2164$01.00/0

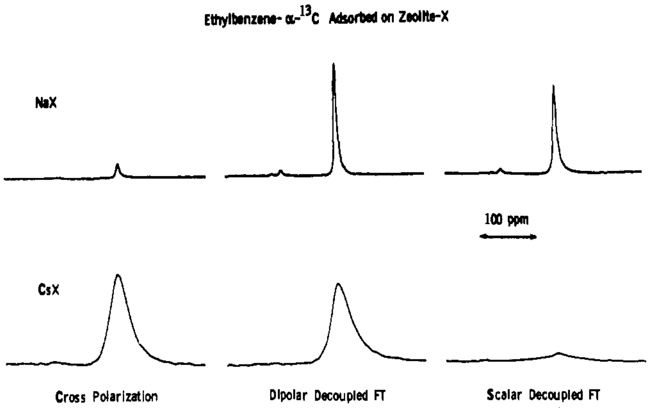

Figure 1. ^{13}C NMR spectra of ethylbenzene-α-^{13}C adsorbed on NaX (top row) and CsX (bottom row), obtained with cross-polarization dipolar-decoupled FT and scalar-decoupled FT techniques (left to right). Contact times of 1 ms were used in the cross-polarization spectra.

the application of a strong radio-frequency field ($\gamma H_2/2\pi$ = 30 kHz) to reduce or eliminate the dipolar magnetic field created by the ^1H-^{13}C dipolar interactions in slow moving molecules. The dipolar FT NMR experiment detects all the molecules accessible to the scalar FT experiment as well as those molecules with components of motion slower than the decoupling field strength, in this case <30 kHz. The third technique used in this study takes advantage of slow molecular motions. In the cross-polarization (CP) experiment the protons are first polarized in the rotating frame and then the polarization is transferred to the carbons via the static component of the dipolar interaction. Since the transfer of polarization is proportional to the static interaction, the CP experiment detects only those molecules with motions having components <30 kHz. (The CP experiment also affords a degree of signal enhancement and therefore integrated areas are not directly comparable to those obtained from the FT experiments.)

Use of either dipolar FT or CP techniques to remove dipolar broadening allows one to observe the chemical-shift dispersion which arises from a chemical-shift anisotropy (CSA) which is not averaged by molecular motion. Interpretation of these chemical shift dispersions in terms of the anisotropic rotation of the molecules has been presented elsewhere.[8,10,20]

Spin-lattice relaxation times (T_1*) were determined from scalar- or dipolar-decoupled partially relaxed Fourier transform spectra obtained from 180°-τ-90° pulse sequences. The T_1* values for the various carbons observed in this study ranged from 100-200 ms when adsorbed on the NaX and from 200-300 ms for the CsX. Single-contact cross-polarization[21] experiments were performed under Hartmann-Hahn[22] conditions ($\gamma_H H_{1H} = \gamma_c H_{1c}$) with contact times between 20 μs and 3 ms. Although the relaxation processes in the cross-polarization experiments were not determined, the slightly diminishing NMR signal at the longest contact times suggests[23] that proton $T_1\rho$ values were on the order of a few milliseconds for molecules adsorbed on these zeolites.

For most samples NMR spectra were recorded under both scalar- and dipolar-decoupled conditions and by cross-polarization techniques over a range of contact times. The spectra displayed in Figures 1-5 were chosen as being representative of the results obtained with each of these experiments or to emphasize a particular feature of the sample. In all cases, the integrated area of the resonances observed with dipolar decoupling was consistent with the amount of carbon-13 known to be in the sample. The ordinates of the spectra in the figures are scaled arbitrarily except where noted. All spectra were recorded at 30 °C.

B. The Samples and Their Preparation. Three catalytic samples were used in this study: NaX, an X zeolite with sodium cations; CsX, an NaX which was exchanged with CsOH at 100 °C; and CsBX, an NaX which was treated with boric acid-CsOH solution at 100 °C.[4,5] Under reaction conditions, the NaX shows poor conversion and poor selectivity as well as producing ring alkylated products.[1] The CsX gives ~60% conversion of the methanol and a selectivity (ratio of styrene and ethylbenzene to methanol consumed) of 40%. The catalysts treated with boric acid, CsBX, give 60% conversion with 50% selectivity.[4]

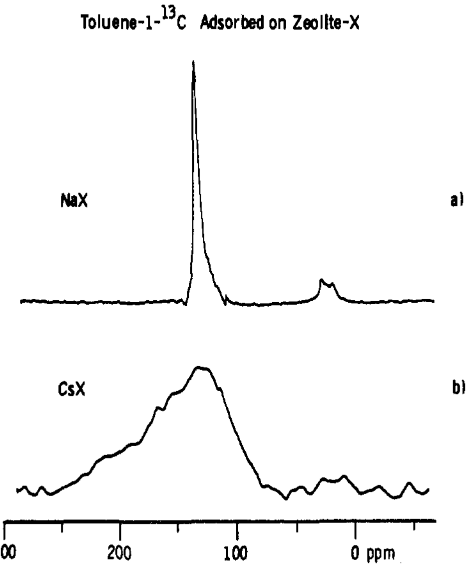

Figure 2. Dipolar-decoupled ^{13}C NMR spectra of toluene-1-^{13}C adsorbed on NaX (top) and CsX (bottom).

All the samples were prepared by dehydrating under vacuum at 420 °C for at least 12 h and then exposing them to the vapors of the isotopically enriched chemicals at room temperature. Toluene-1-^{13}C (90% enriched, Prochem Isotopes) and ethylbenzene-α-^{13}C (90% enriched, Merck & Co.) were used as received except for degassing by freeze-thaw cycles. The samples were allowed to adsorb 20 to 30 mg of substrate/g of zeolite (which corresponds to about one molecule per supercage),[4] the NMR tubes sealed, and spectra recorded without further treatment.

Methanol-^{13}C (90% enriched, Merck & Co.) was handled as described above while paraformaldehyde-^{13}C (90% enriched, Merck & Co.) was preweighed and quickly added to the dehydrated zeolite samples. The sample tubes were again attached to the vacuum system and evacuated at 100 °C for 10 min. The tubes could then be sealed and heated to 200 °C with occasional shaking to allow the paraformaldehyde to volatilize and be adsorbed by the sieve. Typical loading levels of these components were 20-40 mg/g of zeolite. Where experiments required heating of the methanol or formaldehyde, care was taken to vent any noncondensible gases to the vacuum line to prevent a dangerous pressure buildup in the tubes. (Condensible vapors which escaped in this process were returned to the sample tube.)

Results

A. Mobility of Aromatic Adsorbates. Ethylbenzene. The ^{13}C NMR spectra of ethylbenzene-α-^{13}C adsorbed on the NaX are shown in the top of Figure 1. The spectra consist of the predominant resonance of the isotopically enriched methylene carbon which appears at δ_c 29.5 ppm as assigned by comparison with the neat ethylbenzene. The small shoulder on the upfield[24] side of the methylene resonance is due to the natural abundance methyl carbon while the downfield resonances are due to the natural abundance aromatic carbons. The methylene resonance is relatively symmetric, although the line width ($\Delta\nu_{1/2}$ = 120 Hz) is considerably broader than would be observed in a liquid. Application of dipolar decoupling reduces this line width slightly and is easily seen as an increase in the peak height. Cross-polarization techniques produced only a small signal.

Shown at the bottom of Figure 1 are the results of ethylbenzene adsorbed on the CsX which were obtained with the three NMR techniques. On this sample, the scalar-decoupled spectrum was a very broad resonance ($\Delta\nu_{1/2}$ = 1.7 kHz) of low intensity. Dipolar decoupling results in a considerably narrower, asymmetric resonance whose area within the 8-kHz spectral width increased by a factor of 5.6 compared with that of the scalar decoupled spectrum. The cross-polarization spectrum obtained with a 1-ms contact was similar to that obtained with dipolar decoupling.

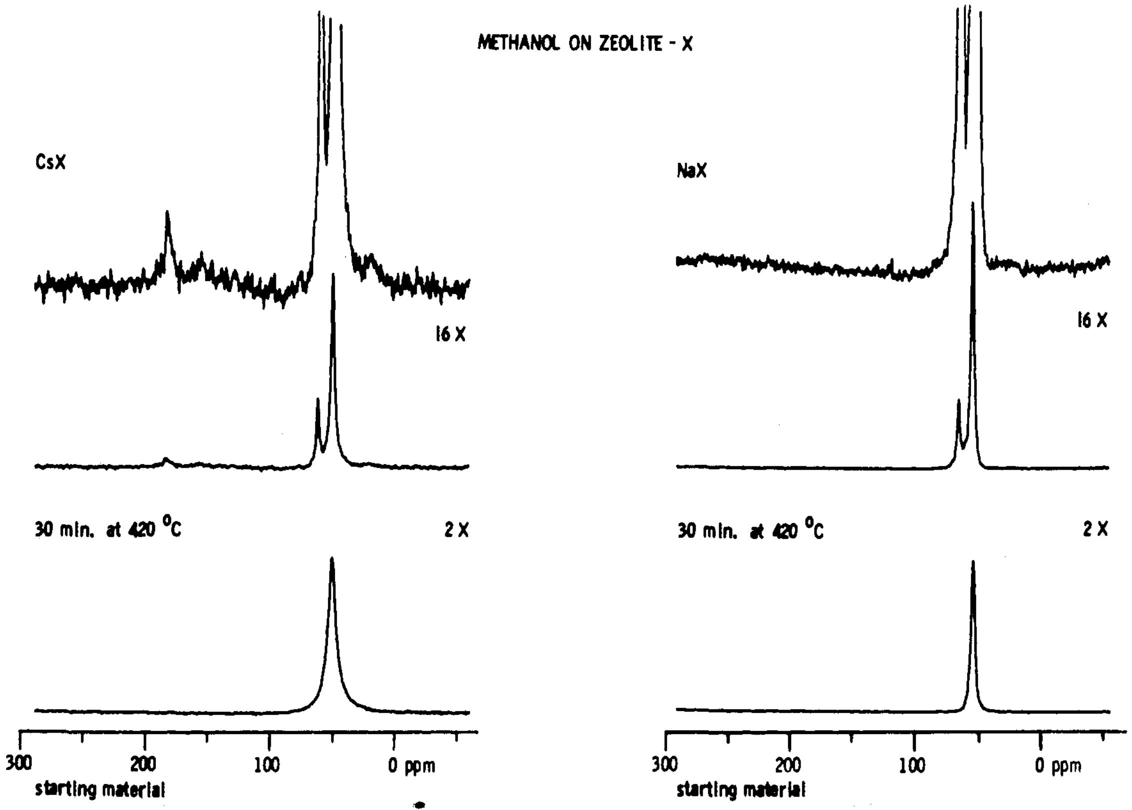

Figure 3. Thermolysis of methanol-^{13}C over NaX (right) and CsX (left). Scalar-decoupled spectra were taken before pyrolysis (bottom row) and after heating to 420 °C for 30 min (middle row). The upper trace has been expanded for clarity.

Toluene. The ^{13}C NMR spectra of toluene-*1*-^{13}C are shown in Figure 2. When adsorbed on the NaX the spectrum consists of a major resonance at δ_c 138 ppm (by comparison with the liquid) due to the isotopically enriched quarternary carbon. As with ethylbenzene adsorbed on this same sieve, the spectral line width is broadened compared with that observed in the liquid. On the CsX a broad chemical-shift dispersion was observed when dipolar interactions were removed by dipolar decoupling. The line width of this resonance indicates that the chemical-shift tensors (arising from the chemical-shift anisotropy) were separated by ~130 ppm. As was observed with ethylbenzene, toluene adsorbed on NaX gave similar spectral intensities with either scalar or dipolar decoupling. In the presence of CsX, however, toluene could be observed only with the aid of dipolar decoupling.

B. Identification of Reaction Intermediates. Methanol. The ^{13}C NMR of 90% isotopically enriched $^{13}CH_3OH$ adsorbed on NaX at 20 mmHg is shown at the bottom right of Figure 3. The sample tube containing the $^{13}CH_3OH$ was heated repeatedly for 15-min intervals at successively higher temperatures and the spectra were recorded after each heat treatment. After the first exposure to 420 °C, a new resonance could be observed at 60.4 ppm which continued to increase in intensity, at the expense of the methanol resonance at δ_c 49.6 ppm, throughout the heating cycles.

Results obtained with the CsX were slightly different. As shown in left of Figure 3, the methanol again appeared at 49.6 ppm and after heating a product appeared at 60.4 ppm. In contrast to the NaX, however, a contribution could also be observed at 183.4 ppm after extensive thermolysis. Cross-polarization spectra indicated the presence of an additional product having a broad symmetric resonance at δ_c 163 ppm.

Formaldehyde. The NMR spectrum of paraformaldehyde appears as a broad symmetric resonance centered at about δ_c 88 ppm whether it is neat or physically mixed with the X-type zeolite as in Figure 4, bottom. The polymeric paraformaldehyde is dissociated by heating at 200 °C and can be readily adsorbed by the zeolites as formaldehyde. In this series of experiments, NMR spectra were recorded after ~10% of the formaldehyde had been adsorbed (usually ~10 min at 200 °C) and then again after heating to 400 °C for 30 min. In the former we hoped to observe adsorbed formaldehyde and in the latter we examined its reaction products.

After adsorption of formaldehyde in the presence of NaX the dipolar-decoupled NMR spectrum contained a peak at 207 ppm in addition to that of the undissociated paraformaldehyde (Figure 4, left). The single-resonance spectrum consisted of only a triplet at 207 ppm with the $^{13}C-^{1}H$ spin-spin coupling constant (J_{CH}) of 183 Hz. Upon further heating at 400 °C the dipolar-decoupled spectrum contained four lines at 182, 124, 60, and 49.5 ppm. Under single-resonance conditions the lines at 182 and 124 ppm remained unchanged while the large signal at 60 ppm appeared as a quartet with J_{CH} = 140 Hz.

The initial spectrum of formaldehyde adsorbed on the CsX showed two resonances of nearly equal intensity with chemical shifts of 162 and 49.5 ppm in addition to that of the paraformaldehyde at 89 ppm (Figure 4, center). Reaction at 400 °C resulted in a dipolar-decoupled spectrum with the major intensity nearly equally distributed between the peaks at 162 and 49.5 ppm and minor contributions at 183, 125, and 60 ppm. Under single-resonance conditions the peak at 49.5 ppm split into a quartet with J_{CH} = 135 Hz. The peaks at 183 and 125 ppm remained unchanged in the single-resonance experiment and the broad peak at 162 ppm was not observed.

When formaldehyde was adsorbed on the borate treated sample, CsBx, the dipolar-decoupled spectrum (Figure 4, right) contained peaks at 207, 183, 88, and 49.5 ppm. (In the single-resonance spectrum the product with a chemical shift of 207 gave a triplet, a singlet remained at 183 ppm, and a quartet appeared at 49.5 ppm.) After 400 °C heating for 30 min, the dipolar-decoupled spectrum contained three relatively narrow lines at 183, 60, and 49.5 ppm. Two broad components,

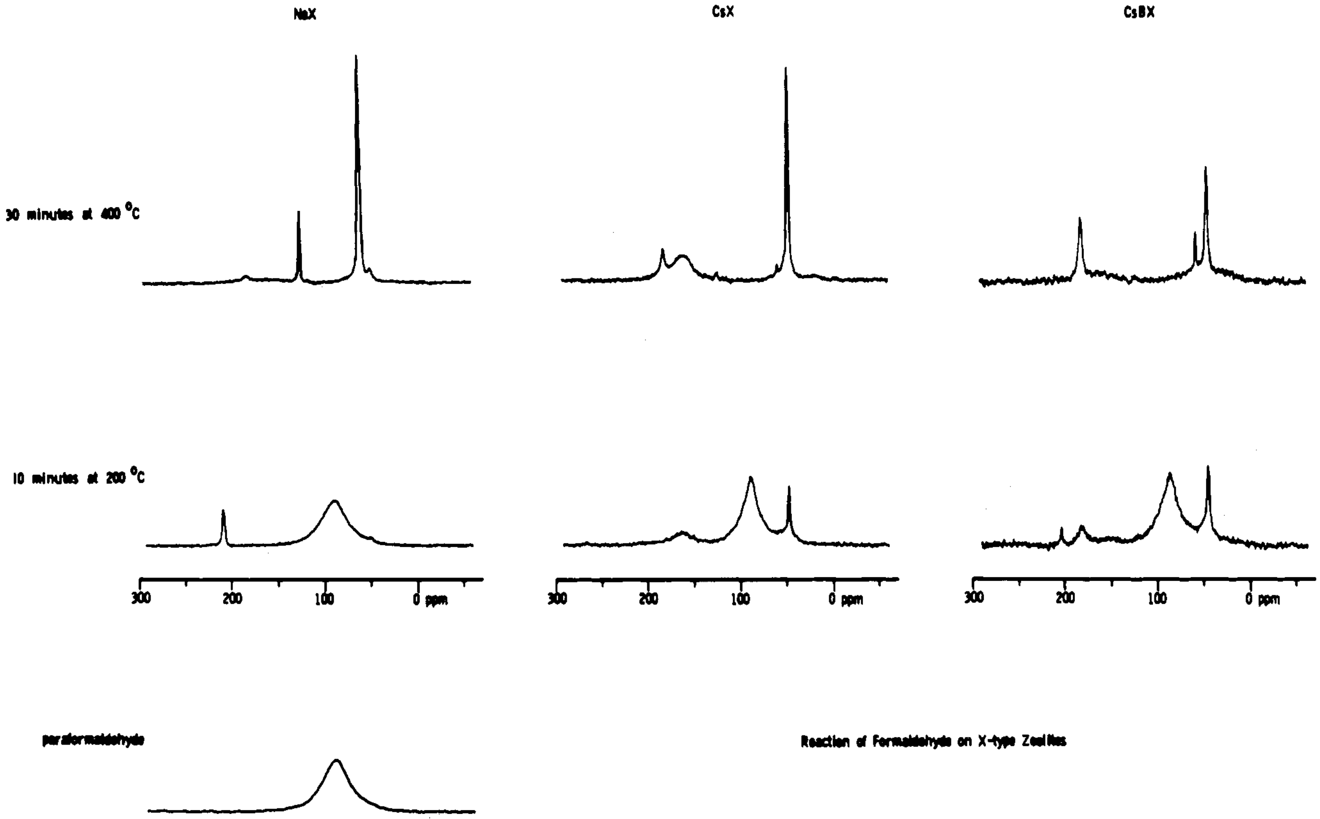

Figure 4. The dipolar-decoupled FT spectra of paraformaldehyde-^{13}C and its pyrolysis products. The center row contains the spectra of the initial adsorption products from the dissociation of paraformaldehyde on NaX, CsX, and CsBX (left to right). Pyrolysis for 30 min at 400 °C results in the spectra shown in the top row.

easily observed with cross-polarization techniques, were centered at 162 and 60 ppm.

Reference Compounds. The ^{13}C NMR of several additional compounds were recorded in order to aid in the identification of reaction products. The chemical shifts and line widths were recorded for each reagent adsorbed at room temperature in 10–30 mg/g of zeolite quantities on both NaX and CsX. Within the accuracy of the chemical-shift measurements here (±2 ppm), no chemical-shift difference was observed between these two zeolites. All chemical shifts reported here were referenced to external standards and no effort was made to correct the observed shifts for the magnetic susceptibility of the sample. The following results were obtained in this laboratory: methanol, 49.5; dimethyl ether, 60; carbon dioxide, 125; formic acid, 163; carbon monoxide, 182 ppm.

Discussion

A. Mobility of Aromatic Adsorbates. The ^{13}C NMR spectra of ethylbenzene-α-^{13}C adsorbed on NaX are shown in the top part of Figure 1. The nearly identical shape and area (within the 8-kHz spectral width) of the scalar and dipolar FT spectra suggest that nearly all (>90%) of ethylbenzene is free to rotate and tumble isotropically at frequencies $>10^5$ kHz. The low intensity and narrow line width of the CP spectrum, when examined over a wide range of contact times, indicate that very little ethylbenzene experiences restricted motion owing to the influence of the molecular sieve.

These results may be contrasted with the bottom of Figure 1, which displays the ^{13}C NMR spectra of ethylbenzene-α-^{13}C adsorbed in CsX. For the CsX the area (within the 8-kHz spectral width) of the scalar FT spectrum is ~1/6 that of the dipolar FT, indicating that >80% of the adsorbed molecules have some components of motion which are slower than ~30 kHz.

In order to verify whether rotation was hindered at the ethyl side chain or the aromatic ring, we investigated the ^{13}C NMR of toluene-*1*-^{13}C adsorbed on these materials. Location of the label on the aromatic ring provides direct indication of the ring mobility. (There is further interest in studying the behavior of the adsorbed toluene as it is a reagent for the styrene synthesis.) The results presented in Figure 2 indicate that toluene behaves as a freely tumbling molecule on the NaX but that considerable inhibition to rotation is encountered on the CsX. These results are consistent with those obtained with ethylbenzene and we believe may be taken to indicate a general trend in the behavior of aromatic adsorbates on these materials.

A more detailed description of the motion of toluene adsorbed on the CsX can be inferred from the NMR line shape. The carbon-13 shielding tensors for toluene have been measured at low temperature[25] and these results, as well as those for other similar aromatic molecules, and presented in Table I.

From the chemical-shift tensors listed in Table I it is possible to predict the shape of the chemical-shift dispersion which would be observed for the various rotational models of toluene. These are given in Figure 5. The experimental data closely match the results predicted for rotation about the C_2 axis of the toluene. We conclude from these results that the adsorbed toluene must relocate by a rotation about its C_2 axis with a frequency greater than $\sim 10^3$ Hz and that any motions which involve rotation about other axes must be much slower than 10^3 Hz. These other motions result in a broadening of the chemical-shift dispersion similar to that observed for CS_2 adsorbed in sodium mordenite.[8] It should be clear that toluene adsorbed on the NaX undergoes rotational reorientation isotropically at a rate faster than 10^5 Hz.

These results on the mobility of adsorbed aromatic molecules, as obtained from NMR measurements, provide a new element of understanding in the behavior of adsorbed mole-

Table I. Carbon-13 Shielding Tensors for Aromatic Molecules

	temp, °C	σ_{11}[a]	σ_{22}[a]	σ_{33}[a]	rotation axis	ref
benzene[b]	−50	186	186	6	C_6	25
hexamethylbenzene[b]	−186	239	161	31	rigid	25
hexamethylbenzene[b]	23	196	196	27	C_6	25
toluene[b]	−186	228	141	3	rigid	25
toluene		184	184	3	pseudo-C_6	calcd[c]
toluene		228	72	72	C_2	calcd[c]
toluene[d]	30	220	90	90	C_2	this work

[a] Units in parts per million relative to Me_4Si. Errors in the shielding tensors are ±1 ppm for benzene, ±6 ppm for hexamethylbenzene and toluene, and ±10 ppm for adsorbed toluene. [b] Neat. [c] Values calculated assuming C_6 rotation averages σ_{11} and σ_{22} and that C_2 rotation averages σ_{22} and σ_{33}. [d] Adsorbed on CsX.

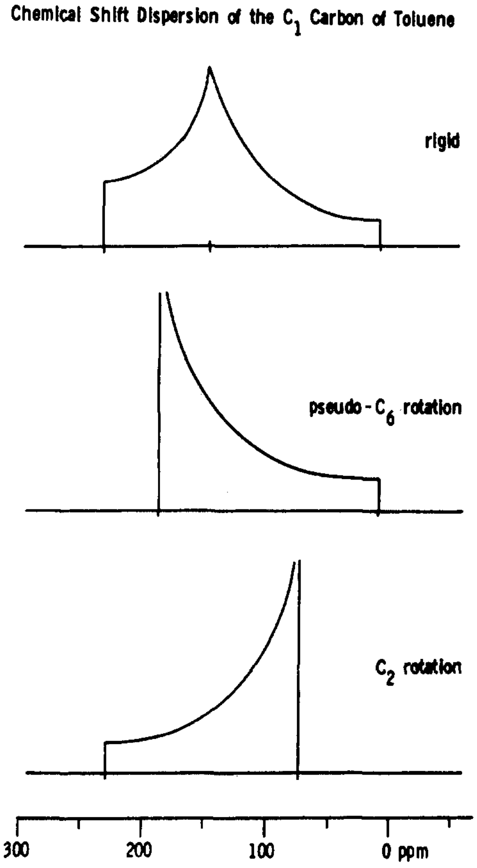

Figure 5. The calculated chemical shift dispersion of the C_1 carbon of toluene in a rigid matrix (top) and as averaged by pseudo-C_6 (middle) and C_2 rotation (bottom) as described in Table I.

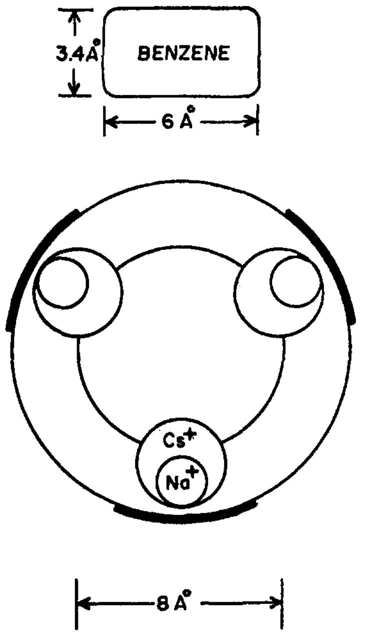

Figure 6. Cross-sectional representation of the X zeolite supercage showing relative cation size and the van der Waals dimensions of benzene.

cules. Previous studies of aromatic molecules adsorbed on X-type zeolites have demonstrated significant perturbation of the π-electron system which was interpreted as being due to the electrostatic fields within the zeolite supercage.[4] Perturbations of the π electrons, as manifested by the ν_1 (ring breathing) vibrational mode and the π–π electronic transition,[5] increase as the size of the cations increases. We interpret our results on the rotational behavior of adsorbed molecules as also being determined by the size of the zeolitic cation. However, we suggest steric rather than electrostatic forces influence the mobility of these adsorbates since the latter decrease with increasing cation size.[26] Figure 6 shows a cross section of the 13 Å adsorption cavity of the X-type sieve. The figure also shows the location of three of the four cations, which reside in the site II position,[27] in the center of the six-membered rings. The cations are illustrated in proportion to their relative ionic radii (Na^+, 0.95 Å, and Cs^+, 1.69 Å).[28] The cesium–cesium separation at the opening of the twelve-membered ring, which interconnects the large cavities, is ~4 Å. The largest sphere which could be placed in the center of the tetrahedrally located cesium ions (i.e., the epicenter of the 13-Å cavity) is ~6.2 Å. (For the sodium ions these distances are 7 and 9 Å, respectively.) Toluene, with dimensions of ~6.7 × 4.0 × 8.6 Å, should be sterically prevented from rotating about its pseudo-C_6 axis and can execute C_2 rotation only in conjunction with translational motion.

It is tempting to suggest a correlation between the inhibition of rotation and catalytic activity. The CsX, which provides the greatest rotational inhibition, is most effective at side-chain alkylation,[1,4] while toluene which rotates freely on the NaX is generally ring alkylated.[2,4] It may be argued that ring alkylation is sterically prevented in the crowded adsorption cavity of the cesium exchanged material. Restricted transition-state selectivity has previously been observed in the transalkylation of alkylbenzenes in the presence of mordenites[29] and the hydrobromination of α olefins catalyzed by CaA.[30] The reduced cavity volume afforded by replacement of the sodium cations with larger cesium ions in X-type zeolites prevents reactions whose transition states require more room than is available in the adsorption cavity. Reactions requiring smaller transition states proceed unhindered. Since the aromatic ring is already severely hindered when it is adsorbed on the CsX (Figures 1, 2), it is unlikely that a transition state involving ring attack could occur within the confines of the molecular sieve cavity.

Transition states involving ring attack must be compatible with the cavity of the sodium sieve since molecules as large as ethylbenzene are able to rotate isotropically without steric hindrance.

B. Identification of Reaction Intermediates. The purpose of this phase of the study was to identify specific reaction intermediates and pathways in the methanol + toluene synthesis of styrene and ethylbenzene and to account for the properties of the alkali metal X-type zeolites which influence that reaction (eq 1).

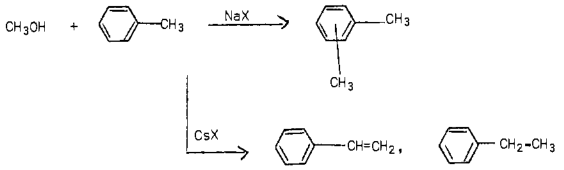

(1)

Sidorenko[3] has proposed that the reaction scheme involves the alkylation of toluene by formaldehyde which is formed by the dehydrogenation of methanol. In support of this proposal, methanol and formaldehyde have been shown to behave similarly in methylating toluene over a wide variety of zeolite catalysts.[1] Unland,[7] noting the similarity in the infrared spectra of adsorbed formaldehyde and decomposed methanol on X-type zeolites, also suggested a common intermediacy in the alkylation of toluene to styrene regardless of whether one starts with formaldehyde or methanol. We have examined the thermolysis of these two methylating agents by NMR in order to provide support for the above proposals and, more importantly, to clarify the role of the alkali cation exchanged zeolites in promoting this reaction.

The scalar-decoupled FT NMR of adsorbed methanol-^{13}C on either NaX or CsX gives rise to a single resonance with no significant chemical shift from the liquid (Figure 3). When either sample was heated for 30 min at 420 °C, a new resonance appeared downfield at δ_c 60.4 ppm. This resonance has been assigned to dimethyl ether on the basis of its chemical shift,[31] the known dehydration properties of NaX[32] and cation-exchanged zeolites,[33] and comparison with the results reported for the decomposition of methanol on a synthetic sodium germanic near-faujasite zeolite (NaGeX).[34] Although the major reaction on both the NaX and CsX was the dehydration of methanol to dimethyl ether, some minor products were also noted. After thermolysis a new resonance appeared in the spectrum of the CsX at δ_c 183 ppm which we have assigned to carbon monoxide on the basis of its chemical shift. The appearance of CO was also associated with the generation of other noncondensible vapors which had to be vented frequently. The noncondensible vapors, which were not analyzed, were presumably H_2, CO, and CH_4 from the dehydrogenation and cracking of methanol. Thermolysis of methanol on the NaX sample produced no detectable CO and little in the way of noncondensible products.

Examination of these samples by cross-polarization NMR provided evidence for one additional product. On the CsX sample cross-polarization spectra with contact times ranging from 0.05-1 ms showed a broad symmetric resonance at δ_c 163 ppm full width at one half maximum height of 770 Hz. The relatively immoble species giving rise to this resonance may be a surface bound formate, a well-known product of methanol decomposition, but positive assignment is withheld in the absence of other evidence. (Formic acid itself has a chemical shift of δ_c 166.3 ppm[31] as a liquid and 163 ppm when adsorbed on X-type zeolites. Ammonium formate appears at 171 ppm,[31] while Derouane[34] has assigned a resonance at 177.1 ppm as belonging to a surface formate in NaGeX. There are three types of formate structure which involve covalent bonding to the surface:[35] monodentate attachment (A) and bidentate attachment through one (B) or two (C) metal centers. Unland has suggested[7] that formate in KX, RbX, and CsX involve the A structure while the bidentate structures B and C are found on NaX. If the tentative assignment of formate to the resonance at 163 ppm is correct, then NMR detection of formate on the NaX might be difficult owing to the added broadening arising from the chemical-shift anisotropy and reduced mobility of the bidentate structure.

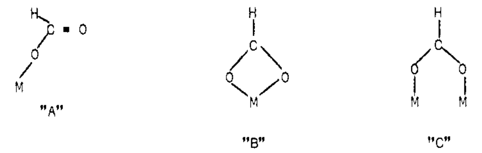

There is no evidence that dimethyl ether from the dehydration of methanol reacts with toluene in the presence of CsX, although over NaX it may result in aromatic alkylation.[33] In either event, there is no evidence that dimethyl ether leads to side-chain alkylation and, as such, is an undesirable byproduct which reduces the overall yield of styrene and ethylbenzene from methanol and toluene.

The NMR spectrum obtained when paraformaldehyde was dissociated in the presence of NaX gave a single new resonance at 207 ppm which we believe is due to unassociated formaldehyde, isolated in the zeolite cavities. We base this assignment on the similarity of the chemical shift with other aldehydes and ketones and on the spin-coupled triplet with J_{CH} = 183 Hz compared with 170 Hz observed in aqueous formaldehyde. To our knowledge this is the first reported chemical shift of free formaldehyde. Heating the sample to 400 °C results in the disappearance of the peaks due to paraformaldehyde and formaldehyde and the appearance of resonances due to dimethyl ether and carbon dioxide at 60 and 125 ppm, respectively. Minor contributions from carbon monoxide and methanol were also observed. These products were identified on the basis of their chemical-shift and spin-spin coupling constants.

Weiss et al.[36] have shown that aqueous base solutions of formaldehyde react at 95 °C over NaX to produce formose sugars and formic acid. Venuto and Landis[14,33] have studied the decomposition of formaldehyde in the gas phase over NaX and at 300 °C the products are given by

$$4CH_2O \xrightarrow[NaX]{300\ ^\circ C} CH_3OCH_3 + 2CO + H_2O \tag{2}$$

In the gas phase at 400 °C we have observed both dimethyl ether and carbon dioxide consistent with the overall reaction given by

$$3CH_2O \xrightarrow[NaX]{400\ ^\circ C} CH_3OCH_3 + CO_2 \tag{3}$$

The observed molar ratio of 2:1 dimethyl ether–carbon dioxide suggests the possibility of other reactions contributing to the production of the ether.

Thermolysis of the paraformaldehyde over the CsX sample lead to entirely different products as determined by the dipolar-decoupled NMR spectrum. At all stages of heating two products, methanol and formate, were observed in near-equal intensity. (These products were identified by comparison of the NMR spectrum with those of authenic samples adsorbed on the zeolite.) After prolonged heating at 400 °C, the presence of carbon monoxide, carbon dioxide, and dimethyl ether was also observed in the NMR spectrum. The simultaneous appearance of both methanol and formate is suggestive of the Cannizzaro reaction (eq 4) which has been previously observed to occur in the presence of NaX zeolites.[33]

$$2CH_2O + OH^- \rightarrow CH_3OH + HCOO^- \tag{4}$$

Dissociation of paraformaldehyde on the borate treated zeolite, CsBX, leads to the appearance of free formaldehyde in addition to carbon monoxide, formate, and methanol as can be seen in the dipolar-decoupled NMR spectrum (see Figure 4). Further heating leads to a large increase in the amount of CO and the appearance of CH_3OCH_3 which were shown previously to be decomposition products of methanol in the presence of CsX. Formate, which we believe is associated with the production of methanol via the Cannizzaro reaction, is more clearly seen in the cross-polarization spectrum as a broad resonance centered at ~160 ppm. The cross-polarization spectrum also indicated the presence of another immobile species which displayed a chemical-shift dispersion near 60 ppm. This latter resonance could be due to a surface-bound methoxide species similar to that observed at 61.6 ppm on the NaGeX zeolite.[34]

The somewhat increased stability of formaldehyde on the borate treated zeolite might be due to the neutralization of some basic sites in the zeolite cavity. The borate may also be responsible for the increased line width of the formate compared with that of the untreated sample. In these studies, however, we have observed no results which would account for the improved catalytic performance of the CsBX sieve.[5]

Conclusions

The results of this study indicated that the zeolite cations in the X-type zeolites affect the alkylation of toluene by chemically controlling the formation of reactive intermediates and byproducts and by sterically influencing the transition-state geometry.

Our results (Figure 3), consistent with the findings of others,[7,33] indicate that dehydration of methanol is favored on NaX while dehydrogenation competes with dehydration on the CsX. Over the NaX formaldehyde is rapidly converted to dimethyl ether (Figure 4) but is converted to methanol by the Cs-exchanged X zeolites at high temperatures. Post-exchange treatment of the CsX with borate affects the removal of excess base, but the catalytic performance[5] of this material seems to us to be greater than inhibition of the Cannizzaro reaction would suggest. No other differences were observed in this study which could account for the improved properties of the CsBX.

In addition to the altering of the catalytic properties of the molecular sieve, we have presented results (Figure 1 and 2) which indicate that the cesium cation may provide a restricted transition-state-type selectivity in the alkylation of toluene. Thus, cesium ions play a twofold role by modifying the nature of the chemical intermediates and preventing unwanted reaction channels by steric inhibition.

Acknowledgment. I thank Dr. Mark Unland for providing the zeolite samples used in this study and am indebted to Dr. Jacob Schaefer for discussion concerning this manuscript.

References and Notes

(1) T. Yashima, K. Sato, T. Hayasaka, and N. Hara, *J. Catal.*, **26**, 303 (1972).
(2) Y. N. Sidorenko and P. N. Galich, *Ukr. Khim. Zh.* (*Russ. Ed.*), **36**, 1234 (1970).
(3) Y. N. Sidorenko, P. N. Galich, V. S. Gutyrya, V. G. Il'in, and I. E. Neimark *Dokl. Akad. Nauk SSSR* **173**, 132 (1967).
(4) J. J. Freeman and M. L. Unland, *J. Catal.*, **54**, 183 (1978).
(5) M. L. Unland, U.S. Patent 4 115 424 (1978).
(6) M. L. Unland and J. J. Freeman, *J. Phys. Chem.*, **82**, 1036 (1978).
(7) M. L. Unland, *J. Phys. Chem.*, **82**, 580 (1978).
(8) M. D. Sefcik, Jacob Schaefer, and E. O. Stejskal, *ACS Symp. Ser.*, **No. 40**, 344 (1977).
(9) M. D. Sefcik and H. K. Yuen, *Thermochima Acta*, **26**, 297 (1978).
(10) S. Kaplan, H. A. Resing, and J. S. Waugh, *J. Chem. Phys.*, **59**, 5681 (1973).
(11) D. Deininger, D. Geschke, and W.-D. Hoffmann, *Z. Phys. Chem.* (*Leipzig*), **255**, 273 (1974).
(12) I. D. Gay and S. Liang, *J. Catal.*, **44**, 306 (1976).
(13) V. Yu. Borovkov, W. K. Hall, and V. B. Kazanski, *J. Catal.*, **51**, 437 (1978).
(14) E. O. Stejskal and Jacob Schaefer, *J. Magn. Reson.*, **14**, 160 (1974).
(15) Jacob Schaefer and E. O. Stejskal, *J. Magn. Reson.*, **15**, 173 (1974).
(16) E. O. Stejskal and Jacob Schaefer, *J. Magn. Reson.*, **18**, 560 (1975).
(17) A. Abragam, "The Principles of Nuclear Magnetism", Oxford University Press, London, 1961.
(18) F. Block, *Phys. Rev.*, **111**, 841 (1958).
(19) Jacob Schaefer, E. O. Stejskal, and R. Buchdahl, *Macromolecules*, **8**, 291 (1975), and references therein.
(20) H. W. Spiess, *Chem. Phys.*, **6**, 217 (1974).
(21) (a) A. Pines, M. G. Gibby, and J. S. Waugh, *J. Chem. Phys.*, **56**, 1776 (1972); (b) *ibid.*, **59**, 569 (1973).
(22) S. R. Hartmann and E. L. Hahn, *Phys. Rev.*, **128**, 2042 (1952).
(23) E. O. Stejskal, Jacob Schaefer, and T. R. Steger, *Faraday Symp., Chem. Soc.*, in press.
(24) All of the NMR spectra presented here are displayed with the field strength increasing from left to right. Chemical shifts are in the δ_c convention, relative to Me_4Si.
(25) A. Pines, M. G. Gibby, and J. S. Waugh, *Chem. Phys. Lett.*, **15**, 373 (1972).
(26) R. M. Barrer and R. M. Gibbons, *Trans. Faraday Soc.*, **61**, 948 (1965).
(27) L. Broussard and D. P. Shoemaker, *J. Am. Chem. Soc.*, **82**, 1041 (1960).
(28) D. W. Breck, "Zeolite Molecular Sieves", Wiley, New York, 1974.
(29) S. M. Csicsery, *ACS Monogr.*, **No. 171**, 680 (1976).
(30) L. C. Fettetly and K. F. Koetitz, *Mol. Sieves, Pap. Conf., 1967*, 102 (1968).
(31) J. B. Stothers, "Carbon-13 NMR Spectroscopy", Academic Press, New York, 1972.
(32) W. J. Mattox, U.S. Patent 3 036 134 (1962).
(33) P. B. Venuto and P. S. Landis, *Adv. Catal.*, **18**, 259 (1968).
(34) E. G. Derouane, P. Dejaifve, and J. B. Nagy, *J. Mol. Catal.*, **3**, 453 (1978).
(35) J. D. Donaldson, J. F. Knifton, and S. D. Ross, *Spectrochim. Acta*, **20**, 847 (1964).
(36) S. Trigerman, E. Biron, and A. H. Weiss, private communication.